J|A|C|S
ARTICLES
Published on Web 07/04/2006

Spectroscopic Characterization of Copper(II) Binding to the Immunosuppressive Drug Mycophenolic Acid

Christopher E. Jones,*[,†,‡] Paul J. Taylor,[||] Alastair G. McEwan,[†,‡] and Graeme R. Hanson[†,§]

Contribution from the Centre for Metals in Biology, School of Molecular and Microbial Sciences, and Centre for Magnetic Resonance, The University of Queensland, St Lucia, Queensland, 4072, and Departments of Medicine, The University of Queensland, and Clinical Pharmacology, Princess Alexandra Hospital, Ipswich Road, Brisbane, QLD 4102, Australia

Received November 10, 2005; Revised Manuscript Received April 24, 2006; E-mail: christopheredward.jones@uq.edu.au

Abstract: Mycophenolic acid (MPA) is a drug that has found widespread use as an immunosuppressive agent which limits rejection of transplanted organs. Optimal use of this drug is hampered by gastrointestinal side effects which can range in severity. One mechanism by which MPA causes gastropathy may involve a direct interaction between the drug and gastric phospholipids. To combat this interaction we have investigated the potential of MPA to coordinate Cu(II), a metal which has been used to inhibit gastropathy associated with use of the NSAID indomethacin. Using a range of spectroscopic techniques we show that Cu(II) is coordinated to two MPA molecules via carboxylates and, at low pH, water ligands. The copper complex formed is stable in solution as assessed by mass spectrometry and ^{1}H NMR diffusion experiments. Competition studies with glycine and albumin indicate that the copper−MPA complex will release Cu(II) to amino acids and proteins thereby allowing free MPA to be transported to its site of action. Transfer to serum albumin proceeds via a Cu(MPA)(albumin) ternary complex. These results raise the possibility that copper complexes of MPA may be useful in a therapeutic situation.

1. Introduction.

Mycophenolic acid (MPA, Chart 1) is a frontline immunosuppressant used for the prophylaxis of rejection following solid organ transplantation. By the late 1990s, over 75% of renal transplant patients in the US were receiving mycophenolate mofetil (MMF), the prodrug of MPA.[1,2] MPA exerts its clinical effect by binding to the active site in the enzyme inosine monophosphate dehydrogenase (IMPDH). This binding inhibits the proliferation of human T and B lymphocytes in two ways. First, IMPDH catalyzes the de novo pathway of guanosine nucleotide synthesis, a pathway that T and B lymphocytes are almost solely dependent upon. Second, MPA inhibits the type II isoform of IMPDH that is expressed in activated lymphocytes, rather than the type I "housekeeping" isoform. Hence MPA is able to selectively inhibit lymphocytes over other cell types.[3,4] IMPDH catalyzes the nicotinamide adenine dinucleotide (NAD) dependent oxidation of inosine-5′-monophosphate (IMP) to xanthosine-5′-monophosphate (XMP). MPA binds to the nicotinamide portion of the NAD binding site after NADH release has occurred but before XMP has been produced. The crystal structure of MPA bound IMPDH shows MPA bound along with an IMP intermediate.[5] All functional groups of MPA are required for binding to IMPDH, including the C2′−C3′ (see Chart 1) double bond which keeps the hexanoic acid side chain in a bent conformation. In addition to IMPDH inhibition, MPA has additional therapeutic effects by inhibiting inducible nitric oxide synthase, an enzyme linked to renal allograft rejection episodes.[4,6]

Chart 1. [a]

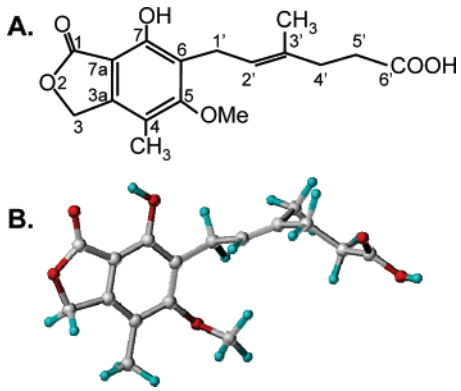

[a] (Panel A) Schematic representation of MPA showing numbering scheme used. (Panel B) Ball and stick model of MPA.

[†] Centre for Metals in Biology.
[‡] School of Molecular and Microbial Sciences.
[§] Centre for Magnetic Resonance.
[||] Departments of Medicine.

(1) Behrend, M.; Braun, F. *Drugs* **2005**, *65*, 1037−1050.
(2) Takemoto, S. K. *Transplant. Proc.* **2002**, *34*, 1632−1634.
(3) Allison, A. C.; Eugui, E. M. *Immunopharmacology* **2000**, *47*, 85−118.
(4) Allison, A. C. *Lupus* **2005**, *14 Suppl 1*, s2−8.
(5) Sintchak, M. D.; Fleming, M. A.; Futer, O.; Raybuck, S. A.; Chambers, S. P.; Caron, P. R.; Murcko, M. A.; Wilson, K. P. *Cell* **1996**, *85*, 921−30.
(6) Senda, M.; DeLustro, B.; Eugui, E.; Natsumeda, Y. *Transplantation* **1995**, *60*, 1143−8.

10.1021/ja057651l CCC: $33.50

Despite many therapeutic benefits, optimal use of MPA has been hampered by a range of side effects. Gastrointestinal (GI) effects are prevalent and in some cases are severe enough to require either cessation or dose changes. Dose changes are known to increase the chance of organ rejection.[1] Oral bioavailability of MPA is increased by administration of the ester prodrug MMF. MMF undergoes rapid hydrolysis to MPA followed by metabolism to MPA glucuronide.[7,8] The rapid hydrolysis of MMF occurs high up in the GI tract and is thought to be partly responsible for the observed GI side effects.[9] In an attempt to combat the adverse effects, an enteric coated formulation of sodium mycophenolate (EC-MPS) was developed.[10] This formulation is designed to dissolve lower down the GI tract at low pH values, hence improving upper GI tolerability. Some cases have indeed shown a remarkable improvement in GI events after the introduction of EC-MPS.[11] Clinical studies have shown this formulation to be therapeutically equivalent to MMF. Despite the enteric coat, the studies have also shown that the overall incidence of adverse events and GI side effects is largely similar between patients on MMF and those on EC-MPS; however the GI severity tended to be lower in the EC-MPS group.[12−14]

Gastrointestinal intolerability is recognized as a significant side effect in the use of many drugs. In particular, the GI effects of aspirin and other nonsteroidal anti-inflammatory drugs (NSAID) are well documented.[15,16] The potent NSAID, indomethacin, has dose-dependent GI side effects in humans and has fatal outcomes if used in dogs.[15] For many years the use of copper to inhibit inflammation has been reported.[15,17,18] Moreover, many reports show that copper complexed NSAIDs are often more effective than the copper salt or the uncomplexed NSAID alone.[17] Significantly, many Cu−NSAID complexes also have greater GI tolerability than the parent NSAID.[15] The GI sparing ability of copper−NSAID complexes is highlighted by copper-bound indomethacin,[19] which has a therapeutic action equivalent to free indomethacin but results in much lower GI damage.[20] Consequently, Cu−indomethacin has found use as an anti-inflammatory in veterinary applications.[15] Copper is the third most abundant transition metal in biological systems (after iron and zinc), and although it is toxic at high concentrations, it is nevertheless attractive for use in therapeutic applications as organisms have very sophisticated mechanisms to sequester and transport the metal. In particular, specific metallochaperones bind copper ions in sites that inhibit deleterious cellular interactions and also transfer the metal to specific copper-requiring enzymes and proteins.[21,22]

Although the pathophysiology of GI intolerance of NSAIDs and MPA is very complex and not clearly understood, it is thought that one of the mechanisms underlying GI toxicity is a direct interaction between the drug and the gastric phospholipids. An electrostatic interaction between negatively charged carboxyl groups on the drug and the positively charged quaternary ammonium group of phosphatidylcholine has been suggested as a mechanism behind NSAID gastropathy.[23] This interaction appears to reduce the ability of surface-active phospholipids to form a hydrophobic protective layer.[23] Such a topical effect may also account for some of the GI effects of MPA, and the effects would only be exacerbated by the rapid hydrolysis of MMF to free-acid MPA. Copper binding to indomethacin occurs via the carboxylate group.[19] The complexation most likely inhibits the ability of the carboxylate to bind to lipid headgroups which may partially explain the observed reduction in GI toxicity.[23] Indomethacin is a nonselective inhibitor of cyclooxygenase (COX). Two isoforms of COX exist; COX-1 has a number of roles including controlling the gastric mucosa, while COX-2 produces the prostaglandins involved in inflammation and mitogenesis. Indomethacin-induced inhibition of COX-1 is thought to play a role in GI ulcerogenic activity. Currently it is unclear if copper−indomethacin plays a role in the COX enzyme system; however, uptake of intact copper−indomethacin complexes has been reported, and the complex remains a potent anti-inflammatory.[15,24] Additionally, the copper−indomethacin complex displayed superoxide dismutase (SOD) activity, which was suggested to contribute to the lower ulcerogenic activity of the copper complex compared to indomethacin alone.[20] SOD is available in the gastric mucosa of the GI tract and is thought to be involved in protecting the gastric and duodenal mucosa from damaging species.[25] Thus, copper−indomethacin may reduce gastric damage via a number of mechanisms.

Based on the observation that enteric-coated MMF results in reduced severity of adverse GI events, combined with the successful use of copper to combat the GI effects of indomethacin and related NSAIDs, we investigated the potential use of this metal ion to coordinate MPA. We have characterized the binding of copper to MPA using a range of spectroscopic techniques including NMR, EPR, and mass spectrometry. Additionally, the affinity of Cu(II) for MPA has been estimated. Further, as MPA is highly bound to serum albumin (97%),[1] and the protein has numerous Cu(II) binding sites, we have investigated the interaction of copper-bound MPA with albumin. The copper−MPA complex formed may be beneficial as an immunosuppressant having reduced GI toxicity.

2. Experimental

2.1. Materials. MPA (*E*-6-(1,3-dihydro-7-hydroxy-5-methoxy-4-methyl-1-oxoisobenzofuran-6-yl)-4-methyl-4-hexanoic acid) was obtained from the Sigma Chemical Co. (St. Louis, MO) and used without

(7) Bullingham, R. E.; Nicholls, A.; Hale, M. *Transplant. Proc.* **1996**, *28*, 925−9.
(8) Johnson, A. G.; Rigby, R. J.; Taylor, P. J.; Jones, C. E.; Allen, J.; Franzen, K.; Falk, M. C.; Nicol, D. *Clin. Pharmacol. Ther.* **1999**, *66*, 492−500.
(9) Holt, C. D.; Sievers, T. M.; Ghobrial, R. M.; Rossi, S. J.; Goss, J. A.; McDiarmid, S. V. *BioDrugs* **1998**, *19*, 373−384.
(10) Rihs, G.; Papageorgiou, C.; Pfeffer, S. *Acta Crystallogr.* **2000**, *C56*, 432−433.
(11) Suwelack, B.; Gabriels, G.; Volmer, S.; Hillebrand, U.; Hohage, H.; Pohle, T. *Transplantation* **2005**, *79*, 987−988.
(12) Salvadori, M.; Holzer, H.; de Mattos, A.; Sollinger, H.; Arns, W.; Oppenheimer, F.; Maca, J.; Hall, M.; Groups, T. E. B. S. *Am. J. Transplant.* **2004**, *4*, 231−236.
(13) Sollinger, H. *Transplant. Proc.* **2004**, *36*, 517s−520s.
(14) Budde, K.; Glander, P.; Diekmann, F.; Dragun, D.; Waiser, J.; Fritsche, L.; Neumayer, H. H. *Transplant. Proc.* **2004**, *36*, 524s−527s.
(15) Weder, J. E.; Dillon, C. T.; Hambley, T. W.; Kennedy, B. J.; Lay, P. A.; Biffin, J. R.; Regtop, H. L.; Davies, N. M. *Coord. Chem. Rev.* **2002**, *232*, 95−126.
(16) Rodriguez, L. *Lancet* **1994**, *343*, 769−772.
(17) Sorenson, J. R. J. *Inflammatory Diseases and Copper*, 1st ed.; Humana Press: Clifton, NJ, 1982.
(18) Sorenson, J. R. J. In *A Physiological Basis for Pharmacological Activities of Copper Complexes, A hypothesis*; Sorenson, J. R. J., Ed. *The Biology of Copper Complexes*; Humana Press: Clifton, NJ, 1987.
(19) Weder, J. E., et al. *Inorg. Chem.* **1999**, *38*, 1736−1744.
(20) Dillon, C. T.; Hambley, T. W.; Kennedy, B. J.; Lay, P. A.; Zhou, Q.; Davies, N. M.; Biffin, J. R.; Regtop, H. L. *Chem. Res. Toxicol.* **2003**, *16*, 28−37.
(21) Harrison, M. D.; Jones, C. E.; Solioz, M.; Dameron, C. T. *Trends Biochem. Sci.* **2000**, *25*, 29−32.
(22) Tottey, S.; Harvie, D. R.; Robinson, N. J. *Acc. Chem. Res.* **2005**, *38*, 775−783.
(23) Giraud, M.-N.; Motta, C.; Romero, J. J.; Bommelaer, G.; Lichtenberger, L. M. *Biochem. Pharmacol.* **1999**, *57*, 247−254.
(24) Lee, S. Y.; Belmonte, A. A. *J. Pharm. Sci.* **1994**, *83*, 1107−9.
(25) Klinowski, E.; Broide, E.; Varsano, R.; Eshchar, J.; Scapa, E. *Eur. J. Gastroenterol. Hepatol.* **1996**, *8*, 1151−5.

further purification. Deuterated water and methanol were obtained from Cambridge Isotopes. During titrations, copper was added as small aliquots from a freshly prepared stock solution of $CuCl_2 \cdot 2H_2O$. Where pH adjustments were required K_2HPO_4/KH_2PO_4 or KOH was used. All chemicals and solvents were AR grade unless otherwise stated and were used without further purification. All experiments were conducted in a range of differing solvent concentrations (e.g., 100% MeOH to 4% MeOH in water) where possible, and the solvent conditions were found to not interfere with the results.

2.2. UV/visible Spectroscopy. UV/visible electronic absorption spectra were obtained on a Cary 3010 spectrometer, using a 1 cm path length cell. All spectra were acquired over a wavelength range from 220 to 1000 nm. Analysis of the λ_{max} of the Cu(II) $d-d$ transitions was undertaken using the method of Billo,[37] updated by Prenesti and co-workers.[38] Briefly, an estimate of the absorption maximum can be calculated with the equation:

$$\lambda_{max} = 10^3/\Sigma_i n_i \nu_I \quad (1)$$

where n_i is the number of each equatorial donor group ($1 \leq n \leq 4$) and ν_i represents the individual contribution of each equatorial ligand to the ligand field of the complex. For a carboxylate oxygen $\nu_i = 0.353 \pm 0.008\ \mu m^{-1}$; water oxygen $= 0.296 \pm 0.006\ \mu m^{-1}$, and hydroxide oxygen = alcoholate oxygen $= 0.39 \pm 0.03\ \mu m^{-1}$.[37,38]

2.3. Electron Paramagnetic Resonance Spectroscopy (EPR). Continuous wave EPR spectra at either ~9.4 GHz (X-Band) or ~4 GHz (S−Band) were obtained on a Bruker Elexsys E500 spectrometer operated with Bruker Xepr software. Spectra were obtained using either a super high-Q or optical cavity (X-band) or a flexline resonator (S-band). Calibration of the magnetic field was achieved using an ER035 gaussmeter. The microwave frequency was calibrated with an EIP548B microwave frequency counter. A Eurotherm B-VT-2000 variable temperature controller provided stable temperatures of ~140 K. Spectra were routinely baseline corrected using polynomial functions and smoothed using Fourier filtering available in the Xepr software. Simulations of the EPR spectra were performed using XSophe (version 1.1.4) running on a Linux workstation. Spectra were routinely simulated using matrix diagonalization for the analysis of randomly oriented EPR samples, starting with experimentally derived g and A matrices.[26]

2.4. Nuclear Magnetic Resonance Spectroscopy (NMR). All NMR spectra were obtained on a Bruker Avance 500 MHz spectrometer using a 5 mm triple-resonance, z-gradient probe. MPA samples were prepared in either d_4-MeOH or 90% D_2O/10% d_4-MeOH. All spectra were acquired at 303 K. If required, the residual water signal was suppressed using either a low power presaturation pulse or a W5 watergate sequence.[27] Proton spectra were generally acquired over a 10 ppm spectral width, with 32K real points, and ^{13}C spectra were acquired over a 200 ppm spectral width. Data were acquired and processed using Bruker Topspin software running on Linux workstations. Generally, the one-dimensional spectra were processed using a $\pi/2$ shifted sine-squared window function. Spectra were referenced to the residual methanol signal at 3.30 ppm (for ^1H spectra) and at 58 ppm (for ^{13}C spectra). Resonance assignments for apo-MPA were determined using 1D ^1H and ^{13}C-DEPT experiments and standard chemical shift tables[28] and were based on those of Makara et al.[29] Diffusion coefficients for apo- and copper-bound MPA in d_4-MeOH were determined using the DOSY program supplied in the Topspin software (Bruker). Pulse field gradient NMR spectra were acquired using a bipolar gradient, stimulated echo sequence. Diffusion coefficients were measured by incrementing the amplitude of the field gradient pulses over 32 steps (0.8−32 G/cm). The duration of the field gradient pulse (10ms) and the diffusion time (200ms) were held constant for all experiments. The spectra were recorded with 32 scans in a 2D mode, and a relaxation delay of 2 s between scans. The gradient strength was calibrated using the diffusion of residual water in a 100% D_2O sample ($\sim 1.9 \times 10^{-9}\ m^2\ s^{-1}$).[30] The Bruker T_1/T_2 relaxation routine was used for all data analysis. Peak intensities were fitted to an exponential decay using the *SimFit* program within the Topspin software to provide estimates of the diffusion constant (D). The hydrodynamic radius (r_s) of MPA and copper-bound MPA were estimated from the Stokes−Einstein equation:

$$D = kT/6\pi\eta r_s \quad (2)$$

(assuming a spherical shape for the molecules), where k is the Boltzmann constant ($1.38 \times 10^{-16}\ g\ cm^2\ s^{-2}\ K^{-1}$), T is the temperature of the experiments (303 K), and η is the viscosity of the solvent (MeOH) at 303 K ($5.1 \times 10^{-3}\ g\ cm^{-1}\ s^{-1}$).

2.5. Mass Spectrometry. All mass spectra were collected on a Perkin-Elmer API III triple quadrupole instrument (PE-Sciex, Thornhill, Toronto, Canada) fitted with an electrospray interface and operated in the positive ionization mode. Spectra were collected at a low (orifice potential 40 V) or high (orifice potential 100 V) energy. Samples were applied via a direct infusion method at a flow rate of 20uL/min. The temperature of the interface was constant at 40 °C, and nitrogen was used as the nebulizer gas. A minimum of 10 scans was collected for each sample. Spectra were processed using MacSpec software (PE Sciex) on a Macintosh computer.

2.6. Competition with Glycine. The competition between MPA and glycine for Cu(II) was monitored by UV/vis spectroscopy. Additions of glycine were made from an aqueous stock solution of 0.05 M glycine. Glycine has an absolute affinity (pH independent) for Cu(II) of $4.3 \times 10^9\ M^{-1}$ and a stoichiometry of 2:1 (gly/Cu(II)).[31] At pH 6.0 the dissociation constant is ~16 μM ($\log \alpha = pK_a - pH = 9.63-6.0 = 3.63$, $\log K_1(app)$ (Cu(II)) $= 8.1-3.63 = 4.47$ or $2.95 \times 10^4\ M^{-1}$).[31]

2.7. Transfer of Cu(II) to Serum Albumin. The competition of bovine serum albumin (BSA) and MPA for Cu(II) was monitored by EPR. MPA (0.8mM) with 1 equiv of Cu(II) was prepared in 99% H_2O/1%MeOH with additions of BSA, from a 1.4 mM solution of BSA in H_2O, to give a final volume of 1 mL. The pH of all MPA solutions was ~6.3. The concentration of BSA was based on an A_{279} (1 mg/mL, 1 cm) = 0.667.[32,33]

3. Results and Discussion

3.1. pH Dependence and Cu(II) Binding by UV/visible Spectroscopy. Using ultraviolet and visible absorption spectroscopy we have investigated the Cu(II) binding to MPA and its pH dependence. The pH dependence of MPA in 99% H_2O/1% MeOH is shown in Figure 1A. As the pH is increased from ~pH 3 to ~pH 9 the spectra show a number of changes. The intensity of the three main low pH transitions observed at approximately 225, 250, and 305 nm all decrease as the pH is increased, and new transitions are observed at approximately 235 and 342 nm. The clear isosbestic points provide evidence for a simple equilibrium, which may simply be the presence of only two absorbing species. The intensities of the 305 and 342 nm peaks are plotted as a function of pH and are shown in the inset to Figure 1A. The intensities of these two peaks are equivalent at ~pH 8.2, which most likely corresponds to the pK_a of the phenolic group of MPA. The species in solution are

(26) Hanson, G. R.; Gates, K. E.; Noble, C. J.; Griffin, M.; Mitchell, A.; Benson, S. *J. Inorg. Biochem.* **2004**, *98*, 903−916.
(27) Lui, M.; Mao, X.; Ye, C.; Huang, H.; Nicholson, J. K.; Lindon, J. C. *J. Magn. Res.* **1998**, *132*, 125−129.
(28) Abraham, R. J.; Fisher, J.; Loftus, P. *Introduction to NMR spectroscopy;* John Wiley and Sons: New York, 1988.
(29) Makara, G. M.; Keseru, G. M.; Kajtar-Peredy, M.; Anderson, W. K. *J. Med. Chem.* **1996**, *39*, 1236−42.
(30) Longsworth, L. G. *J. Phys. Chem.* **1960**, *64*, 1914−1917.
(31) Dawson, R. M. C.; Elliot, D. C.; Elliot, W. H.; Jones, K. M. *Data for Biochemical Research*, 3rd ed.; Clarendon Press: Oxford, 1986.
(32) Sadler, P. J.; Tucker, A.; Viles, J. H. *Eur. J. Biochem.* **1994**, *220*, 193−200.
(33) Janatova, J.; Fuller, J. K.; Hunter, M. J. *J. Biol. Chem.* **1968**, *243*, 3612−22.
(34) Buzzeo, M. C., et al. *Inorg. Chem.* **2004**, *43*, 7709−25.

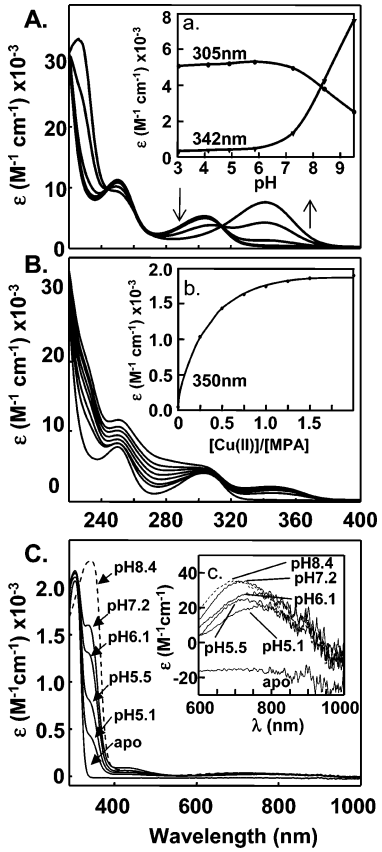

Figure 1. UV/visible spectra of Cu(II) binding to MPA. (Panel A) pH titration of apo-MPA in 99%H_2O/1%MeOH. MPA (0.1 mM) was titrated with K_2HPO_4 from pH 4.8 to pH 9.2. Inset a shows the absorbance at 305 and 342 nm plotted as a function of pH. (Panel B) Cu(II) titration of 0.1 mM MPA in 100%MeOH. Cu(II) was added in 0.25 mol equiv until a maximum of 2 equiv had been added. Inset b shows the absorbance at 350 nm plotted as a function of mole equivalents of copper added. (Panel C) pH titration of 0.5mM [CuMPA] in 96% H_2O/4% MeOH. Inset c shows Cu(II) $d-d$ transitions as a function of pH.

likely to be the carboxylate anion at low pH values and the carboxylate and the phenolate anion at pH values > 8.5.

The titration of MPA with Cu(II) in MeOH is shown in Figure 1B. As Cu(II) is titrated into a solution of MPA a new band becomes apparent at ~350 nm. Weak transitions around 350 nm have been observed in many copper complexes and have been attributed to square-pyramidal [CuO_4O] complexes,[19] and CuO_4 centers in [$Cu(OAr)_4$] complexes.[34] In the latter case, the transition is considered $d-d$ in origin. Increases are also observed in the range 230−300 nm, which may be due to Cu(II)-carboxy charge transfer absorption that usually occurs between 240 and 280 nm.[35] The inset in Figure 1B shows the absorption at 350 nm plotted as a function of the Cu(II) equivalents. The absorption at 350 nm tends to plateau after 1 equiv of Cu(II) has been added. However, the stoichiometry is difficult to ascertain due to the lack of a distinct point at which the plateau begins, suggesting weak binding or the presence of multiple species. Indeed, the Cu(II) titration (Figure 1B) shows no isosbestic points that would indicate formation of a single copper-bound species.

Peaks due to Cu(II) transitions were also observed in the visible region at ~450 nm (giving the solution a pale yellow color) and at ~750 nm. A pH titration of MPA with 1 mol equiv of Cu(II) bound (Figure 1C) shows that the pH affects many of the transitions. As the pH increases, the peaks at 350, 450, and 750 nm all increase in intensity. At pH 8.4 the 350 nm peak overlaps with transitions due to the phenolate anion as observed in Figure 1A. The peak initially at 750 nm (shown inset Figure 1c) shows a steady hypsochromic shift, moving to ~690 nm at pH 8.4. The λ_{max} of the $d-d$ bands is largely dependent on the nature of the equatorial ligands.[36,37] At low pH (pH 5.1) the $d-d$ transitions observed in this work occur at a wavelength near 750 nm. Using the method of Prenesti et al.,[38] based on that of Billo[37] (eq 1) the predicted λ_{max} of a single Cu(II) bound to two carboxylate groups and two water ligands would be ~770 nm, which corresponds favorably with the pH 5.1 λ_{max} (~750 nm) observed in Figure 1c. As the pH increases to around 7, the λ_{max} moves to ~700 nm which could represent Cu(II) coordinated to carboxylates and a mixture of water and hydroxide ligands. Beyond this pH the λ_{max} moves below 700 nm, suggesting the ligands coordinated to the Cu(II) ion involve carboxylate and either alcoholate or hydroxide moieties. Possibly, the coordination at high pH involves contributions from the phenolate anion.

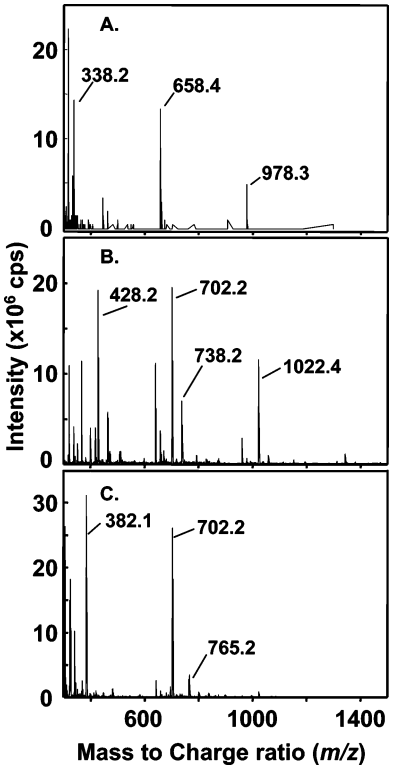

Figure 2. Mass spectrometric analysis of Cu(II) binding to MPA. (Panel A) Spectrum obtained for MPA (1 mM) at pH 5 in 99%H_2O/1%EtOH. The orifice potential was 40 V. Major peaks labeled correspond to MPA ammonium adducts. (Panel B) Spectrum obtained for MPA (1 mM) loaded with 1 mol equiv of Cu(II) at pH 5 (99%H_2O/1%EtOH) at low orifice potential (40 V). (Panel C) Same sample as that for Panel B, but spectrum was recorded with a high orifice potential (100 V).

3.2. Copper−MPA Complexes by Mass Spectrometry. The electrospray mass spectra of apo- and Cu(II)-bound MPA are shown in Figure 2. The spectrum of apo-MPA (Figure 2A)

(35) Dendrinou-Samara, C.; Jannakoudakis, P. D.; Kessissoglou, D. P.; Manoussakis, G. E.; Mentzafos, D.; Terzis, A. *J. Chem. Soc., Dalton Trans.* **1992**, *22*, 3259−3264.

(36) Bryce, G. F.; Gurd, F. R. *J. Biol. Chem*. **1966**, *241*, 1439−1448.

(37) Billo, R. J. *Inorg. Nucl. Chem. Lett.* **1974**, *10*, 613.

(38) Prenesti, E.; Daniele, P. G.; Prencipe, M.; Ostacoli, G. *Polyhedron* **1999**, *18*, 3233−3241.

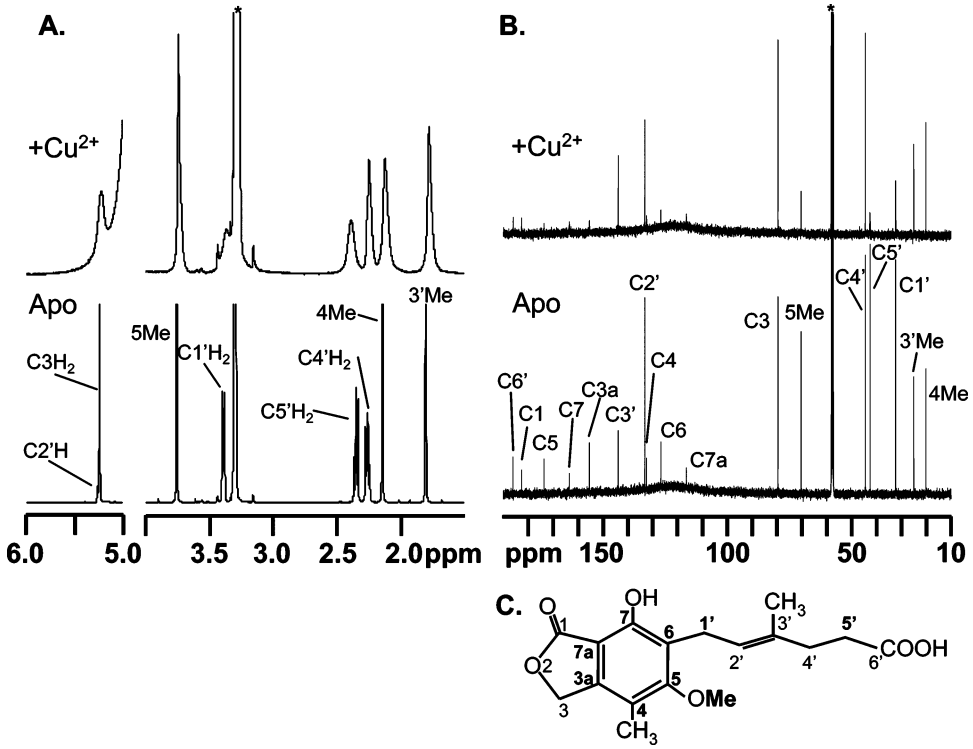

Figure 3. A 500 MHz NMR analysis of Cu(II) binding to MPA. A small aliquot (~0.2 mol equiv) of Cu(II) was added to MPA (~2 mM) in d_4-MeOH at 300 K. (Panel A) ^{1}H NMR spectra of apo-MPA (bottom trace) and [CuMPA] (top trace); (Panel B) ^{13}C NMR spectra of apo-MPA (bottom trace) and [CuMPA] (top trace); and (Panel C) schematic of MPA with positions in bold highlighting of ^{13}C atoms perturbed by addition of paramagnetic Cu(II). Resonance assignments are based on those of Makara et al.[29] * indicates solvent peaks.

shows that MPA (MW = 320.3 g/mol) exists in this solution (~90%H_2O/10%EtOH) as a mixture of monomer ($[MPA + NH_4]^+$, *m*/*z* 338.2), dimer ($[MPA_2 + NH_4]^+$, *m*/*z* 658.4) and some trimer ($[MPA_3 + NH_4]^+$, *m*/*z* 978.3). These masses reflect the formation of ammonium ion adducts as a result of residual contaminating buffer in the electrospray interface. Addition of Cu(II) (as $CuCl_2$) results in the disappearance of the *m*/*z* 338.2, 658.4, and 978.3 peaks and the appearance of a new set at predominantly *m*/*z* 702.2 and 1022.4, as shown in Figure 2B. The *m*/*z* 702.2 peak is most likely two MPA molecules after the loss of two labile carboxylic acid protons and the addition of the Cu(II) ion ($[Cu(MPA)_2 - 2H]^+$). The peak at *m*/*z* 1022.5 involves formation of $[Cu(MPA)_2 - 2H]^+$ followed by addition of a neutral MPA molecule ($[Cu(MPA)_2 - 2H + MPA]^+$), although it is unknown if the additional MPA molecule is a copper ligand. A mass spectrum acquired with 2 mol equiv of Cu(II) shows no change to the ratio of the *m*/*z* 702.2 and 1022.4 peaks which suggests that the third MPA molecule is not involved as a copper ligand (data not shown). Indeed, association between MPA molecules is observed in the spectrum of apo-MPA. Analysis of the *d*−*d* transitions in Figure 1c suggested that, at the pH of the mass spectrometry experiments (pH 5), the predominant Cu(II) complex involved carboxylate and water ligands. Analysis of Figure 2B shows a peak at *m*/*z* 738.2 representing $[Cu(MPA)_2 - 2H + 2H_2O]^+$, confirming the UV/vis analysis. The observation of this peak, even at low orifice potentials (40 V), is unexpected as fragmentation during electrospray ionization can lead to a loss of solvent molecules and, at higher orifice potentials, may even result in ligand dissociation.[39,40] The fact that any *m*/*z* 738.2 molecular ion is observed is testament to the stability of the Cu(II) complex. Further coordination from solvent molecules is also observed at *m*/*z* 428.4 ($[CuMPA - 2H + C_2H_5OH]^+$). Chloride ion does not appear to be involved in any of the major complexes formed. At a very high orifice potential (100 V) the spectrum shows complete loss of all solvent bound complexes and $[Cu(MPA)_3]^+$ (Figure 2C), but retention of $[Cu(MPA)_2]^+$ and production of a copper bound monomer ($[CuMPA - 2H]^+$, *m*/*z* 382.0) and a low abundance binuclear, dimeric species ($[Cu_2MPA_2 - 2H]^+$, *m*/*z* 765.0). This result shows that $[Cu(MPA)_2]^+$ is one of the most stable species. The mass spectroscopic data show that there is heterogeneity in the type of Cu(II) complexes formed, providing a rationale as to why the stoichiometry is difficult to determine from the UV/visible data alone.

3.3. Structural Analysis by ^{1}H and ^{13}C NMR. Figure 3A shows the ^{1}H NMR spectra obtained for apo-MPA and after a small amount of Cu(II) has been added. Cu(II) is a d^9 ion that is paramagnetic irrespective of the coordination geometry (for mononuclear complexes). The paramagnetic nature of Cu(II) tends to broaden all MPA resonances to some extent; however, some peaks show a greater affect upon Cu(II) binding than others. The broadening of resonances can occur as a result of through-bond (contact) or through-space (pseudo-contact) interactions. Typically, pseudo-contact effects only occur over short distances (<7 Å). Despite some general broadening, C1′H_2, C2′H_2, and C5′H_2 all show greater perturbation than, for instance, the methyl groups. Specific broadening of the C5′H_2 protons is expected due to Cu(II) coordination to the carboxylate, but broadening of C1′ and C2′ protons of the hexanoic side

(39) van den Brenk, A. L.; Byriel, K. A.; Fairlie, D. P.; Gahan, L. R.; Hanson, G. R.; Hawkins, C. J.; Jones, A.; Kennard, C. H. L.; Moubaraki, B.; Murray, K. S. *Inorg. Chem.* **1994**, *33*, 3549−3557.
(40) van den Brenk, A. L.; Fairlie, D. P.; Gahan, L. R.; Hanson, G. R.; Hambley, T. W. *Inorg. Chem.* **1996**, *35*, 1095−1100.

chain suggests they are in close proximity to the Cu(II) ion. The hexanoic side chain has a restricted conformation due to the presence of the C7 hydroxy and C5 methoxy groups on the aromatic ring and the *E* geometry of the side-chain double bond. NMR analysis of apo-MPA in solution suggested that the most likely stable solution configuration involves a bent conformation with the carboxyl group bent toward the aromatic ring rather than being in an extended conformation (although C4′ to the end of the chain is the most conformationally flexible region).[29] If the bent conformation is retained in the Cu(II) complex, then the copper ion will be closer to C1′ and C2′ than other groups. The protons of the C5 methoxy group (5Me) are not too perturbed suggesting this group is not close to the metal ion despite the apparent closeness to C1′ and C2′. Makara et al. show that the methoxy group is forced out of the plane of the aromatic ring as a result of interactions with the neighboring methyl and hexanoic acid groups.[29] In apo-MPA the NMR derived distance between the C5 methoxy group and the C1′ and C2′ protons is 4.0 Å and 3.3 Å, respectively. These distances suggest that, even with the Cu(II) ion being close to C1′ and C2′ protons, the C5 methoxy protons will be on the margin of observable paramagnetic broadening.

The ^{13}C spectra (Figure 3B) show predominantly C1′H$_2$, C5′H$_2$, and the C5 methoxy group all having a decrease in intensity upon Cu(II) coordination. The atoms most affected by the addition of Cu(II) are highlighted in bold in Figure 3C. If the broadening of the C′5 resonance is due to the effect of the Cu(II) ligating via the carboxyl group (the C6′ resonance also shows a distinct intensity effect in the ^{13}C spectrum), then the dramatic effect on C1′ and nearby atoms is due to their being within the 7 Å pseudo-contact range. The C2′ carbon atom does show a decreased intensity upon Cu(II) binding; however the effect is less pronounced than the effect to the C1′ carbon atom. Interestingly, all carbons from the aromatic, phenolic group of MPA show a decrease in intensity upon Cu(II) binding. This is likely to result from an interaction of the Cu(II) ion with the delocalized electrons of the aromatic ring. Ligation of the copper ion via the carboxylate group, with the hexanoic side chain in a bent conformation that places the Cu(II) ion within range of C1′ carbon and hydrogen atoms and the C2′ protons, would also locate the ion relatively close to the aromatic ring electrons. Although the protons of the C5 methoxy group show limited perturbation in the ^{1}H NMR spectrum (Figure 3A), the C5 methoxy carbon atom (5Me) displays a reduction in ^{13}C intensity. Rather than implying an involvement in the coordination of copper, it is likely that the reduced intensity is due to an inductive effect as a result of perturbation of the aromatic ring protons via the attached oxygen. Possibly, such an effect also contributes to the observed effects on the atoms of C1′ and C2′ groups of the side chain, although similar effects are not seen at C1, C3, or the C4 methyl group. Coordination of the Cu(II) via the oxygen atom on C1 can be ruled out (due to limited effect on the C1 intensity in the ^{13}C NMR spectrum); however the general perturbation to aromatic ring protons makes it more difficult to discount involvement of the C7 hydroxy group using NMR data alone. The low pH UV/visible data tend to rule out the C7 hydroxy group as a direct, equatorial ligand; however, it is possible it plays a role in stabilizing the Cu(II) ion via a distant, axial interaction.

Although the paramagnetic nature of Cu(II) causes broadening of resonances in ^{1}H NMR experiments, diffusion coefficients have been determined for Cu(II) complexes from such spectra.[41] Diffusion coefficients obtained here for apo-MPA and copper-bound MPA were 9.7×10^{-10} m^2/s and 7.7×10^{-10} m^2/s, respectively (Supporting Information, Figure S1). These values correspond to an apparent hydrodynamic radius of 4.4 Å and 5.6 Å for apo- and copper-bound MPA, respectively (eq 2). The increase in the radius of copper-bound MPA compared to apo-MPA suggests that specific copper−MPA complexes are stable in solution and confirms that the broadening is not just a general result of paramagnetic Cu(II) in solution.

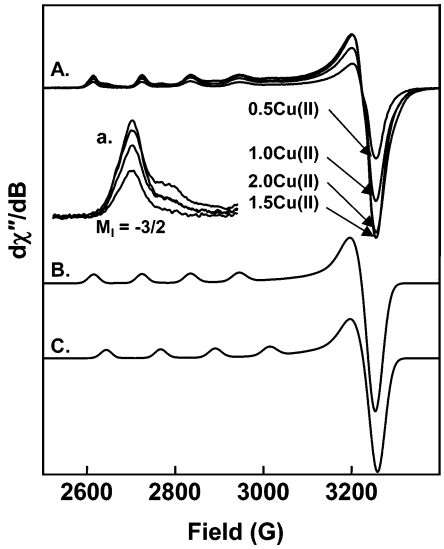

Figure 4. Cu(II) binding titration of MPA (1 mM) in 90% H_2O/10% MeOH, pH ∼5, monitored by X-band EPR spectroscopy ($\upsilon = 9.428\,411$). (A) Spectra obtained as MPA was titrated with 0.5 mol equiv of Cu(II) to a maximum of 2 mol equiv. Inset a highlights the $M_I = -3/2$ resonance showing the minor species apparent beyond ∼0.5 mol equiv of Cu(II). (B) Computer simulation (XSophe) of the EPR spectrum from the major species ($[Cu(MPA)_2(H_2O)_2]$). (C) Computer simulation (XSophe) of the EPR spectrum from the minor species.

3.4. Coordinating Ligands by EPR. The EPR spectra obtained upon titration of MPA with Cu(II) are shown in Figure 4A. The spectra reveal a characteristic axially symmetric Cu(II) center. Titration of up to 2 equiv of Cu(II) results in an increase in the parallel (e.g., $M_I = -3/2$ copper hyperfine resonance, inset to Figure 4A) and perpendicular resonances until a plateau is reached at 1.5 equiv. However, beyond ∼0.5 equiv a second, minor set of resonances is observed (Figure 4A and inset). Computer simulation (XSophe[26]) of the EPR spectra giving rise to the major and minor sets of resonances with the axially symmetric g and $A(^{63}Cu)$ hyperfine matrices listed in Table 1 yield the spectra shown in Figure 4B and 4C, respectively (line width parameters[26] for the simulations are provided as Supporting Information S4). The g and A matrices (Table 1) for the major and minor copper-bound MPA species are similar to those obtained for tetragonally distorted Cu(II) complexes in which the four equatorial ligating atoms are oxygen.[44] Comparison of the EPR and mass spectroscopic data suggests that the major EPR active Cu(II) species is associated with the mononuclear MPA dimer ($[Cu(MPA)_2(H_2O)_2]^+$), while the minor species may be due to complexes involving solvent molecules. Although not undertaken for this study, advanced EPR techniques such as HYSCORE (orientation selective

(41) Ramadan, S.; Hambley, T. W.; Kennedy, B. J.; Lay, P. A. *Inorg. Chem.* **2004**, *43*, 2943−2946.

Table 1. Spin Hamiltonian Parameters for the Cu(II) MPA and BSA Complexes

complex	$g_{\|}$	$g_{\perp}$	$A_{\|}^a$ (^{63}Cu)	$A_{\perp}^a$ (^{63}Cu)	$A_{\|}^a$ (^{14}N)	$A_{\perp}^a$ (^{14}N)	reference
$[Cu(MPA)_2(H_2O)_2]^b$	2.423	2.086	124.00	10.00			this work
Cu−MPA (minor species)	2.381	2.086	137.00	10.00			this work
[Cu(MPA)(BSA) ternary complex^c	2.322	2.062	156.00	13.80	12.89	13.2	this work
[CuBSA] (site I)^d	2.177	2.055	217.00	13.00	12.20	13.00	ref 42
[CuBSA] (site II)	2.24	2.02	165.00	*e*	*e*	*e*	ref 43

^{a} Units for ^{63}Cu hyperfine coupling constants are 10^{-4} cm^{-1}. ^{b} Major species. ^{c} There are three magnetically equivalent nitrogen nuclei coordinated to the Cu(II) ion. ^{d} There are four magnetically equivalent nitrogen nuclei coordinated to the Cu(II) ion. ^{e} Values not given.

hyperfine sublevel correlation spectroscopy) would enable a more detailed evaluation of the species present. EPR spectra obtained at S-band frequencies (Supporting Information, Figure S2) reveal the presence of only a single species. Computer simulation of the S-band (ca. 4 GHz) spectrum with an axially symmetric spin Hamiltonian yielded parameters consistent with those found for $[Cu(MPA)_2(H_2O)_2]^+$ measured at X-band (ca. 9 GHz). Presumably, the reduced *g*-value separation prevented the observation of the minor species, even though the line widths were narrower at S-band, a consequence of the distribution of *g*- and *A*-values.

Binding of copper to indomethacin[19] and acetate[45] results in formation of a binuclear copper center ligated to four indomethacin/acetate groups which are in a "paddle-wheel" type arrangement. These complexes have a Cu−Cu separation of ∼2.6 Å (for indomethacin) which is readily observable in EPR measurements. Although we observed a binuclear complex in the mass spectrum acquired at an orifice potential of 100 V (Figure 2C) and a weak apparent $\Delta M_S = \pm 2$ resonance centered at $g_{eff} = 4.3$ was observed in the X-band EPR spectrum (data not shown), we were unable to simulate both the $\Delta M_S = \pm 1$ and $\Delta M_S = \pm 2$ resonances assuming a dipole−dipole coupled binuclear Cu−Cu center. In addition, such a species was not supported by the S-band EPR spectrum. We concluded that the observed resonance ($g_{eff} = 4.3$) was due to small amounts of adventitious Fe^{3+} and that under normal conditions formation of a binuclear Cu(II) complex does not occur.

3.5. Copper Affinity: Competition with Glycine. The competition of copper-bound MPA with glycine provides insight into the apparent affinity of Cu(II) for MPA. The Cu−glycine complex has an apparent dissociation constant of ∼16 μM at the pH at which these experiments were conducted (∼pH 6.0).[31] Glycine coordinates copper via the amine nitrogen and the carbonyl oxygen, and two glycine amino acids are required to coordinate a single copper ion. Figure 5A shows the increase in absorbance at 350 nm observed during the titration of MPA with Cu(II). As glycine is titrated the 350 nm absorption is lost as the amino acid abstracts Cu(II) from the copper−MPA complex (Figure 5B). This result shows that glycine is readily able to remove Cu(II), so that by the time a stoichiometric amount of glycine has been added the absorbance at 350 nm is at a baseline level similar to that seen for apo-MPA; i.e., all copper has been removed from MPA. The dissociation constant of MPA and Cu(II) is therefore likely to be greater than 16 μM (the K_d of glycine at pH 6.0). The dissociation constant of

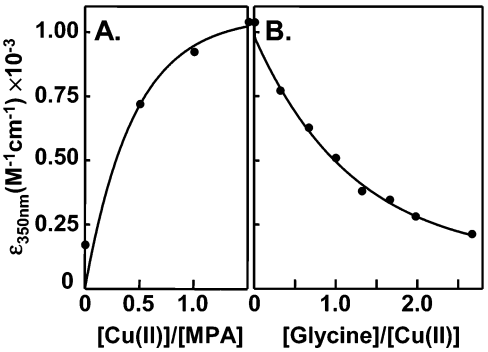

Figure 5. Competition between [CuMPA] and glycine. Panel A shows the absorbance at 350 nm plotted as a function of Cu(II) equivalents added during a titration of 0.1 mM MPA (99%H_2O/1%MeOH, pH 5.8) with Cu(II). Panel B shows the absorbance at 350 nm plotted as a function of equivalents of glycine titrated (relative to Cu(II)). A glycine/Cu(II) ratio of 2:1 represents stoichiometric glycine.

copper-bound acetic acid at pH 6 (assuming a stoichiometry of 2:1, acetic acid/Cu(II)) is ∼550 μM,[31] and a dissociation constant near this for MPA would explain the results in Figure 5. A competitive metal ion capture experiment similar to the glycine competition described here, but with acetic acid as the competitor, showed that copper-bound MPA (including minor species) was able to resist abstraction by acetic acid over a range of pH values (from ∼pH 5 to pH 6.1). Further, analysis of the mass spectrum obtained after the addition of copper, stabilized as copper-acetate, to apo-MPA showed that the most predominant peaks were at *m*/*z* 702.2 ($[Cu(MPA)_2 - 2H]^+$) and *m*/*z* 428.0 (CuMPA−solvent adduct) (Figure S3, Supporting Information). These results confirm that MPA has a higher affinity for copper than does acetic acid but is much less than that of glycine, a simple amino acid.

3.6. Formation of a [Cu(MPA)(BSA)] Ternary Complex and Sequestration of Cu(II) by BSA. Therapeutically, MPA is a very specific and effective inhibitor of IMPDH, and generally, attempts to improve the efficacy by altering functional groups result in a less active drug. Therefore it is desirable that the carboxylate group be prevented from interacting with the lipid headgroups, to minimize adverse GI effects, but that free MPA is able reach the site of action and interact with IMPDH. To this end Cu(II) has to dissociate from MPA prior to binding to its target enzyme, IMPDH. MPA is highly bound to serum albumin (97%),[1] and the protein has at least two Cu(II) binding sites (denoted here as $Cu_{(A)}$, $Cu_{(B)}$) including a strong N-terminal site that binds Cu(II) in a square-planar geometry via four nitrogen ligands ($Cu_{(A)}$), which is similar in both human and bovine albumin.[32,42,46] Figure 6 shows the EPR spectra obtained when BSA is added to solutions of copper-bound MPA. The addition of 0.5 mol equiv (i.e., ∼stoichiometric for Cu(II) assuming two Cu^{2+} sites) of BSA (Figure 6B) results in a

(42) Rakhit, G.; Antholine, W. E.; Froncisz, W.; Hyde, J. S.; Pilbrow, J. R.; Sinclair, G. R.; Sarker, B. J. *J. Inorg. Biochem.* **1985**, *25*, 217−224.
(43) Pandeya, K. B.; Patel, R. N. *Indian J. Biochem. Biophys.* **1992**, *29*, 245−250.
(44) Peisach, J.; Blumberg, W. E. *Arch. Biochem. Biophys.* **1974**, *165*, 691−708.
(45) Mathey, Y.; Greig, D. R.; Shriver, D. F. *Inorg. Chem.* **1982**, *21*, 3409−3413.
(46) Zgirski, A.; Frieden, E. *J. Inorg. Biochem.* **1990**, *39*, 137−48.

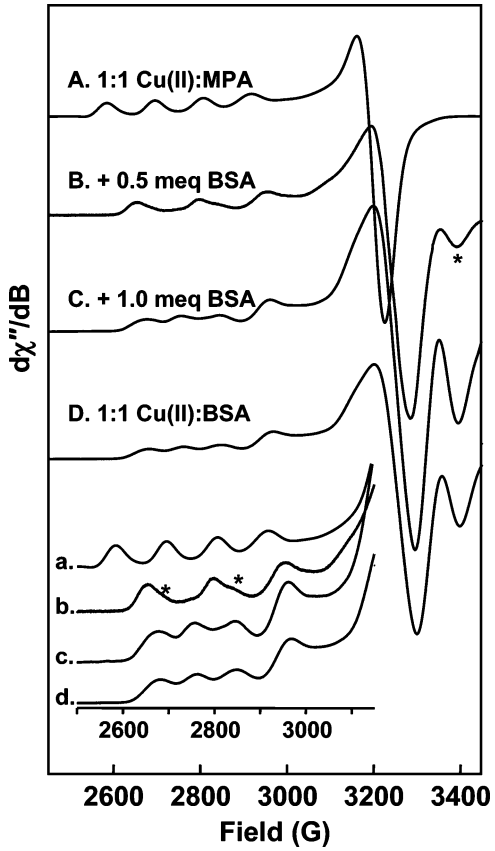

Figure 6. Transfer of copper from [CuMPA] to BSA monitored using EPR. EPR spectra were obtained for (A) copper-bound MPA (0.8 mM, pH 6.3), $\nu = 9.3444$ GHz, $T = 130$ K; (B) after addition of 0.5 mol equiv of BSA, $\nu = 9.340\ 22$ GHz, $T = 70$ K; (C) after addition of 1.0 mol equiv of BSA and (D) copper-bound BSA (0.35 mM, pH 6.5), $\nu = 9.3606$. Insets a−d highlight the parallel region of each spectrum. * highlights resonances from [CuBSA].

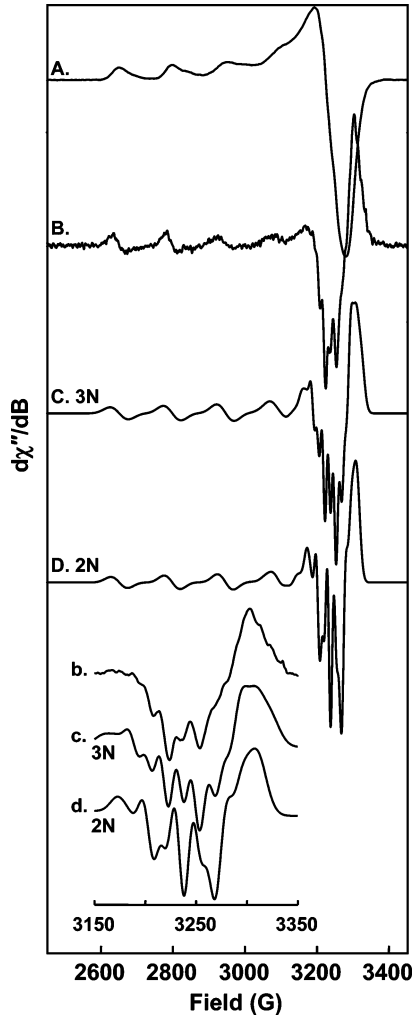

Figure 7. EPR spectra of the ternary [Cu(MPA)(BSA)] complex. (A) The first derivative EPR spectrum obtained by subtracting the spectrum of [CuBSA] (Figure 6D) from that of [CuMPA] to which 0.5 equiv had been added (Figure 6B). $\nu = 9.340\ 22$ GHz, $T = 70$ K. (B) Second derivative EPR spectrum. (C) Computer simulation of Figure 7B assuming three magnetically equivalent nitrogen nuclei and (D) computer simulation of Figure 7B assuming two magnetically equivalent nitrogen nuclei. Insets b−d show an expansion of the perpendicular regions of the spectra shown in Figure 7B−D, respectively.

spectrum with two components; the major species is clearly different to both [CuMPA] (Figure 6A) and a 1:1 Cu^{2+}/BSA complex (Figure 6D), especially in the parallel region (Figure 6, inset a−d). The minor species (resonances labeled with an "*") corresponds to the spectrum of the 1:1 Cu^{2+}/BSA complex (confirmed through spectral subtraction after correcting for small differences in microwave frequencies), and this was found to increase upon aging the solution for approximately 1 week. There is no evidence of copper-bound MPA after the addition of 0.5 equiv of BSA, which suggests both major Cu(II) sites in BSA are filled (i.e., formation of [$Cu_{(A)}Cu_{(B)}$BSA]). Addition of 1 equiv of BSA (Figure 6C) results in a spectrum that is indistinguishable from the spectrum of copper-bound BSA (Figure 6D and inset d) suggesting all Cu(II) has been sequestered from copper-bound MPA. Presumably the 1:1 Cu^{2+}/BSA complex largely represents copper bound to the strong, N-terminal site, i.e., [$Cu_{(A)}$BSA], but it is quite likely that exchange occurs between the copper sites in BSA.

Subtraction of the EPR spectrum of [$Cu_{(A)}$BSA] (Figure 6D) from the spectrum of [CuMPA] with 0.5 equiv of BSA (Figure 6B) yields the spectrum attributable to the ternary complex, Figure 7A. The second derivative of this spectrum is shown in Figure 7B. The perpendicular region of this spectrum (Figure 7b) clearly shows the presence of nitrogen hyperfine coupling indicating that [CuMPA] forms a ternary complex with BSA (MPA has no nitrogen groups). Computer simulation of this spectrum (Figure 7B and b) with the spin Hamiltonian parameters in Table 1, and an axially symmetric spin Hamiltonian assuming three or two magnetically equivalent nitrogen nuclei yields the spectra shown in Figure 7C and 7D, respectively. A comparison of the experimental (b) and simulated (c, d) insets reveals that the simulation based on three magnetically equivalent nuclei (Figure 7c) is in better agreement with the experimental spectrum (Figure 7b) than that that for two (Figure 7d) magnetically equivalent nuclei. Ternary adducts between chelated metals and albumin are not unprecedented[43,47] and are thought to occur at the preferential copper binding site in BSA in which the copper(II) ion is coordinated by four nitrogen nuclei. While the binding of bismaltolato oxovanadium (BMOV) to human serum albumin involves equatorial ligation of a histidine imidazole and peptide nitrogen atoms,[47] the ternary [Cu(MPA)(BSA)] complex has a N3O donor set in the equatorial plane arising from three nitrogen atoms in BSA and the carboxylate oxygen from MPA. In contrast to the binding of

(47) Liboiron, B. D.; Thompson, K. H.; Hanson, G. R.; Lam, E.; Aebischer, N.; Orvig, C. *J. Am. Chem. Soc.* **2005**, *127*, 5104−5115.

BMOV to human serum albumin, the formation of the ternary complex does not depend on the order of addition of Cu(II), MPA, and BSA.

4. Conclusions

It is clear from the spectroscopic analysis presented herein that Cu(II) complexes of MPA are formed over a wide range of pH values, even at the low pH values expected in the GI tract. The spectroscopic data indicate that the type of complex formed when MPA binds Cu(II) is pH dependent. At low pH values (~5), such as may be encountered in the GI tract, the copper ion is ligated via two oxygen atoms from carboxylate groups (unidentate coordination) and two water ions to form a mononuclear MPA dimer, $[Cu(MPA)_2(H_2O)_2]^+$. The lower intestine has a higher pH than the stomach, and there it is possible that the copper−MPA complex has alcoholate or hydroxide groups in place of the water ligands. Mass spectrometry and NMR diffusion experiments confirm that the copper−MPA complex is stable in solution. It is likely that the Cu(II) complex retains the bent hexanoate side-chain conformation observed for apo-MPA (see Chart 1). Due to the bent conformation, hindered dynamics, and consequent bulky nature of MPA, it is probable that the two MPA ligands adopt a *trans* configuration around the Cu(II) ion rather than a *cis* geometry. Steric considerations also provide a rationale as to why higher order species are not abundant and/or stable. In the presence of BSA, $[Cu(MPA)_2(H_2O)_2]^+$ loses the water ligands along with an MPA molecule to form a ternary complex. Formation of a ternary complex provides a mechanism for the transport of MPA to the site of action, whereupon an excess of BSA, or other copper(II) sequestering proteins, releases MPA allowing it to exert its clinical effect. The major species formed in this work can be interpreted by the following equilibria:

$$\begin{array}{rcl} \mathrm{Cu(II)} + 2\mathrm{MPA} & \overset{K_1}{\rightleftharpoons} & [\mathrm{Cu(MPA)_2(H2O)_2}]^+ \\ [\mathrm{Cu(MPA)_2(H2O)_2}]^+ + \mathrm{BSA} & \overset{K_2}{\rightleftharpoons} & [\mathrm{Cu(MPA)(BSA)}] + \mathrm{MPA} \\ & & \Big\Updownarrow K_3 \\ & & [\mathrm{Cu(BSA)}] + 2\mathrm{MPA} \end{array} \quad (3)$$

Our results indicated that aging the solution in the presence of BSA results in complete abstraction of Cu(II) from $[Cu(MPA)_2(H_2O)_2]^+$, and therefore $K_3 > K_2$. Although this work shows that Cu(II) will be lost to albumin, it is also possible that the metal may be lost earlier to enzymes and proteins found in the GI tract. In this respect copper-bound MPA may act similarly to EC-MPS; however, instead of a slowly dissolving coat, the loss of Cu(II) leaves free MPA to exert a clinical effect. This also leaves Cu(II) to either be absorbed and utilized or excreted. The low pH of the stomach would result in greater loss of copper compared to the increased pH of the lower intestine. Indeed, copper−indomethacin has a greater effect in the lower GI tract compared to the stomach, although the copper-bound drug was less damaging in both areas than indomethacin alone.[20] Gastrointestinal intolerability is one of the limiting factors in optimal MPA use. GI damage can occur due to a number of factors including direct topical irritation to the GI epithelium, impaired barrier properties (e.g., binding to phospholipids), suppression of prostaglandin synthesis, and interference with the repair mechanism after superficial injury.[15] In the case of MPA, further GI toxicity may arise due to the antiproliferative effect of the drug on enterocytes.[1] Importantly, however, the reduced severity of GI effects observed with EC-MPS suggests that a direct topical interaction is a contributing factor. Although much further physiologic investigation is required, the characterization of the copper mycophenolate complex provided here suggests that it may find a place in the arsenal of immunosuppressive therapy. To this end, investigations into the interactions of MPA and copper-bound MPA with synthetic phosphocholine bilayers are currently underway.

Acknowledgment. C.E.J. is the recipient of a C.J. Martin Fellowship from the National Health and Medical Research Council of Australia. Dr. Charles Dameron is thanked for the initial supply of MPA, and Dr. Tri Le is thanked for NMR assistance.

Supporting Information Available: Figure S1 shows a representative intensity versus NMR gradient field strength plot used to obtain diffusion coefficients of copper-bound MPA. Figure S2 shows the S-band EPR spectrum for copper-bound MPA along with the computer simulation of the experimental spectrum. Figure S3 shows the UV/vis and mass spectrometry competitive metal ion capture experiments conducted with acetic acid. S4 is a table of line width parameters for the major and minor copper-bound MPA simulations shown in Figure 4. S5 lists the full authorship of cited articles with >10 authors. This material is available free of charge via the Internet at http://pubs.acs.org.

JA057651L